Probing the Abilities of Synthetically Useful Serine Proteases To Discriminate between the Configurations of Remote Stereocenters Using Chiral Aldehyde Inhibitors

Taekyu Lee and J. Bryan Jones*

Contribution from the Department of Chemistry, University of Toronto, 80 St. George Street, Toronto, Ontario, Canada M5S 1A1

Received August 17, 1995[⊗]

Abstract: The abilities of the synthetically useful serine proteases, subtilisin Carlsberg (SC) and α-chymotrypsin (CT), to discriminate between *R*- and *S*-configurations of stereocenters remote from the catalytic site have been explored using chiral aldehyde transition state analog inhibitors as probes. The inhibitors evaluated were (*R*)- and (*S*)-3-phenylbutanal and (*R*)- and (*S*)-4-phenylpentanal, for which the stereocenters at C-3 and C-4 respectively are distant from the aldehyde functionality that interacts with the catalytic serine residue. The achiral parent compounds, 3-phenylpropanal and 4-phenylbutanal, respectively, were also assessed for reference purposes. Each aldehyde was found to be a competitive inhibitor for both enzymes, with CT being significantly more potently inhibited than SC. Within this series, the presence of an *R*-center methyl group improved binding significantly over that of the achiral parent aldehyde for both enzymes. In contrast, the effects on binding of *S*-methyl substituents in the same positions were modest, and generally somewhat deleterious. Furthermore, the greater the separation of the stereocenter from the aldehyde group, the lower the degree of configuration discrimination. The most effective inhibition, and the highest degree of remote stereocenter discrimination, observed was that by CT of (*R*)-3-phenylbutanal, whose K_I of 8.4 μM was 61-fold lower than that of its achiral parent 3-phenylpropanal, and 88-fold lower than the K_I of its *S*-enantiomer. Molecular mechanics and molecular dynamics calculations were performed to identify each favored aldehyde−enzyme complex and to reveal the binding and orientation differences responsible for the *R*- and *S*-enantiomer binding discriminations observed.

Introduction

Enzymes have now gained general acceptance as chiral catalysts in asymmetric synthesis.[1] In almost all of these cases, the stereocenter being introduced or selected is adjacent to the site of catalysis. Very few examples have been reported where the stereocenter of interest is three or more bonds removed from the carbonyl group of the ester function undergoing hydrolysis.[2] The paucity of examples of stereocenter control remote from enzyme's catalytic sites parallels the situation in non-enzyme catalyzed asymmetric synthesis, where control of the configurations of stereocenters remote from a chiral auxiliary or catalyst represents a major problem that has not yet been solved.[3] However, in enzymatic catalysis, since the whole of an enzyme's active site region that envelopes a substrate in the enzyme−substrate (ES) complex is chiral, discrimination of any substrate stereocenter is feasible in principle, no matter how remotely such a stereocenter is located from the catalytic site. At present, it is not clear whether the meagerness of the database in this regard is due to the fact that enzymatic discrimination of a remote stereocenter is intrinsically difficult or simply that too few examples have yet been sought. These questions cannot be answered at this time because our knowledge of the factors controlling and determining enzyme stereospecificity are still poorly understood. Accordingly, for full advantage to be taken of the synthetic potential that enzymes offer, it is important to identify and to extend our understanding of the factors controlling substrate and inhibitor binding, and it is toward this goal that the present study is targeted.

With synthetic applications of esterases and related hydrolytic enzymes being of such widespread current interest,[1] two serine proteases, subtilisin Carlsberg (SC, EC 3.4.21.14) and α-chymotrypsin (CT, EC 3.4.21.1), were selected as representative hydrolases for our initial studies on remote stereocenter stereospecificity. SC and CT are commercially available enzymes that have been applied in a wide range of synthetic transformations[4] and for which high-resolution X-ray crystal structures are

[⊗] Abstract published in *Advance ACS Abstracts,* December 15, 1995.

(1) (a) Wong, C.-H., Whitesides, G. M. *Enzymes in Synthetic Organic Chemistry*; Pergamon: New York, 1994. (b) *Preparative Biotransformations*; Roberts, S. M., Ed.; Wiley: New York, 1993. (c) *Biotransformations in Preparative Organic* Chemistry; Faber, K., Ed.; Springer-Verlag: Heidelberg, 1992.

(2) (a) Hughes, D. L.; Bergan, J. J.; Amato, J. S.; Bhupathy, M.; Leazer, J. L.; McNamara, J. M.; Sidler, D. R.; Reider, P. J.; Grabowski, E. J. J. *J. Org. Chem.* **1990**, *55*, 6252. (b) Ladner, W. E.; Whitesides, G. M. *J. Am. Chem. Soc.* **1984**, *106*, 7250. (c) Jones, J. B.; Marr, P. W. *Tetrahedron Lett.* **1973**, 3165. (d) Mohr, P.; Waespe-Sarcevic, N.; Tamm, C.; Gawronska, K.; Gawronski, J. K. *Helv. Chim. Acta* **1983**, *66*, 2501. (e) Cohen, S. G.; Weinstein, S. Y. *J. Am. Chem. Soc.* **1964**, *86*, 725.

(3) (a) Ojima, I. *Catalytic Asymmetric Synthesis*; VCH: New York, 1993. (b) Noyori, R. *Asymmetric Catalysis in Organic Synthesis*; Wiley: New York, 1994. (c) Koskinen, A. *Asymmetric Synthesis of Natural Products*; Wiley: New York, 1993. (d) Hegedus, L. *Transition Metals in the Synthesis of Complex Organic Molecules*; S. University Science Books: Mill Valley, CA, 1994.

(4) (a) Delinck, D. L.; Margolin, A. L. *Tetrahedron Lett.* **1990**, *31*, 3093. (b) Pugniere, M.; San Juan, C.; Previero, A. *Tetrahedron Lett.* **1990**, *31*, 4883. (c) Gotor, V.; Garcia, M. J.; Rebelleo, F. *Tetrahedron Asymmetry* **1990**, *1*, 277. (d) Margolin, A. L.; Delinck, D. L.; Whalon, M. R. *J. Am. Chem. Soc.* **1990**, *112*, 2849. (e) Chenevert, R.; Desjardins, M.; Gagnon, R. *Chem. Lett.* **1990**, 33. (f) Chenevert, R.; Letourneau, M.; Thiboutot, S. *Can. J. Chem.* **1990**, 960. (g) Frigerio, F.; Coda, A.; Pugliese, L.; Lionetti, C.; Menegatti, E.; Amiconi, G.; Schnebli, H. P.; Ascenzi, P.; Bolognesi, M. *J. Mol. Biol.* **1992**, *225*, 107. (h) Tsukada, H.; Blow, D. M. *J. Mol. Biol.* **1985**, *184*, 703. (i) Birktoft, J. J.; Blow, D. M. *J. Mol. Biol.* **1972**, *68*, 187. (j) Blevins, R. A.; Tulinsky, A. *J. Biol. Chem.* **1985**, *260*, 4264. (k) Ricca, J. M.; Crout, D. H. *J. Chem. Soc., Perkin Trans. 1* **1989**, 2126. (l) Kitaguchi, H.; Fitzpatrick, P. A.; Huber, J. E.; Klibanov, A. M. *J. Am. Chem. Soc.* **1989**, *111*, 3094. (m) Brieva, R.; Rebelleo, F.; Gotor, V. *Chem. Comm.* **1990**, 1386. (n) Gutman, A. L.; Meyer, E.; Kalerin, E.; Polyak, F.; Sterling, *J. Biotechnol. Bioeng.* **1992**, *40*, 760. (o) Roper, J. M.; Bauer, D. P. *Synthesis* **1983**, 1041.

0002-7863/96/1518-0502$12.00/0

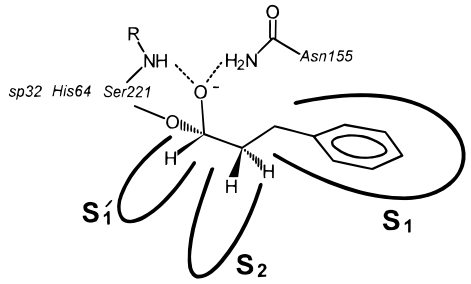

Figure 1. Schematic representation of the EI complex formed when a transition state analog aldehyde inhibitor such as $C_6H_5CH_2CH_2CHO$ (**1**) binds at the active site of subtilisin Carlsberg. Nucleophilic attack of the carbonyl group of **1** by the side chain OH of the serine residue of the catalytic triad Ser221−His64−Asp32 gives the tetrahedral, transition state-like, structure shown, whose anion is stabilized by the amide functions of Asn155 and Ser221 that comprise the "oxyanion hole". The phenethyl group is located in the non-polar S1-pocket, in accord with the dominance of the structural specificity of the enzyme by such hydrophobic interactions. S2 is where the peptide chain binds and S1′ is where the alcohol moiety of ester binds.

available.[5] These serine proteases have an extended active site binding region composed of several subsites, of which the S_1[6] -pocket dominates, particularly in the binding of hydrophobic groups.

For systematic probing of enzyme specificity, evaluating the binding affinities of transition state analog competitive inhibitors[7] represents a convenient strategy, and kinetic studies on boronic acid inhibitors of this type, coupled with graphics analyses and molecular modeling, have been successfully used for the systematic probing of the structural and electrostatic specificity of the S_1-site of SC.[8] This strategy is continued in this paper, using aldehydes as inhibitors. Aldehydes are well known to be transition state analog competitive inhibitors of serine proteases,[9] as illustrated in Figure 1. In this study, the enantiomeric aldehydes (***R***)- and (***S***)-**2,4,** with remote stereocenters positioned either β or γ to the aldehyde, together with the achiral parent structures **1,3** as reference compounds, have been used to evaluate the remote stereocenter stereoselectivity potential of the S_1 pockets of SC and CT and to further probe the structural specificity of these sites.

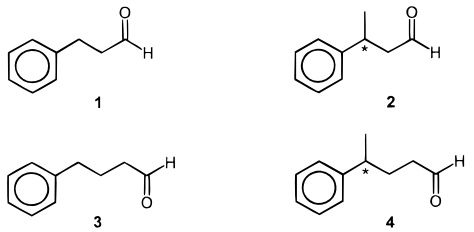

(5) (a) McPhalen, C. A.; James, M. N. G. *Biochemistry* **1988**, *27*, 6582. (b) Bode, W.; Papamokos, E.; Musil, D. *Eur. J. Biochem.* **1987**, *166*, 673. (c) Frigerio, F.; Coda, A.; Pugliese, L.; Lionetti, C.; Menegatti, E.; Amiconi, G.; Schnebli, H. P.; Ascenzi, P.; Bolognesi, M. *J. Mol. Biol*. **1992**, *225*, 107. (d) Tsukada, H.; Blow, D. M. M *J. Mol. Biol*. **1985**, *184*, 703. (e) Birktoft, J. J.; Blow, D. M. M. *J. Mol. Biol*. **1972**, *68*, 187. (f) Blevins, R. A.; Tulinsky, A. *J. Biol. Chem.* **1985**, *260*, 4264. (g)Tulinsky, A.; Blevins, R. A. *J. Biol. Chem.* **1987**, *262*, 7737.

(6) (a) Schechter, I.; Berger, A. *Biochem. Biophys. Res. Commun.* **1967**, *27*, 157. (B) Berger, A.; Schechter, I. *Philos. Trans. R. London, Ser. B* **1970**, *257*, 249.

(7) (a) Lienhard, G. E. *Science* **1973**, *180*, 149. (b) Wolfenden, R. V. *Acc. Chem. Res.* **1972**, *5*, 10. (c) Koehler, K. A.; Lienhard, G. E. *Biochemistry* **1971**, *10*, 2477. (d) Wolfenden, R. V.; Radzicka, A. *Curr. Opin. Struct. Biol.* **1991**, *1*, 780.

(8) (a) Keller, T. H.; Seufer-Wasserthal, P.; Jones, J. B. *Biochem. Biophys. Res. Commun.* **1991**, *176*, 401. (b) Seufer-Wasserthal, P.; Martichonok, V.; Keller, T. H.; Chin, B.; Martin, R.; Jones, J. B. *Bioorg. Med. Chem.* **1994**, *2*, 35.

Table 1. Inhibition of Subtilisin Carlsberg and a-Chymotrypsin by Aldehydes[a]

Inhibitor	α-Chymotrypsin K_I (mM)	Subtilisin Carlsberg K_I (mM)
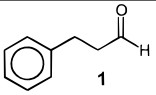 **1**	0.51 ± 0.12 (0.38)[b]	8.41 ± 0.67
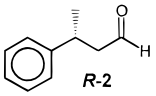 ***R*-2**	0.0084 ± 0.0021	0.53 ± 0.04
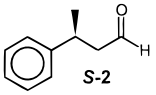 ***S*-2**	0.74 ± 0.18	9.31 ± 0.74
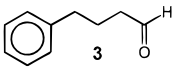 **3**	0.15 ± 0.04	5.36 ± 0.43
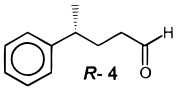 ***R*- 4**	0.068 ± 0.017	0.61 ± 0.05
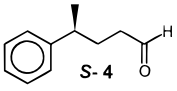 ***S*- 4**	0.86 ± 0.21	2.95 ± 0.24

[a] K_I values for both enzymes were determined[12] in duplicate at pH 7.5 at 25 °C in 0.1 M NaH_2PO_4, 0.5 M NaCl, 0.25 mM of substrate, 5% DMSO in volume, inhibitor concentrations in the range of 5.9−9.1 mM, and enzyme concentrations 4.5 nM (SC) and 16 nM (CT). [b] Data obtained[9a] at 25 °C and pH 7.7 ± 0.3.

Results and Discussion

The aldehyde structures **1**−**4** were selected as suitable structures for S_1-site interaction on the basis of graphics analyses using the X-ray structures of SC and CT.[5] The starting material for the chiral aldehydes was commercially available (±)-3-phenylbutanoic acid, which was resolved into its *R*- and *S*-enantiomers by recrystallizations of its diastereomeric salts with (*R*)- and (*S*)-α-phenethylamines. The methyl esters of the resolved acids were then reduced and the alcohols obtained oxidized, using the Dess−Martin reagent,[10] to the corresponding aldehydes (***R***)- and (***S***)-**2**. The homologous aldehydes (***R***)- and (***S***)-**4** were obtained similarly from the enantiomers of methyl 4-phenylpentanoate obtained *via* Arndt−Eistert homologations[11] of the above (*R*)- and (*S*)-3-phenylbutanoic acids. The achiral reference inhibitor 3-phenylpropanal (**1**) was commercially available, while 4-phenylbutanal (**3**) was prepared from purchased 4-phenylbutanol by Dess−Martin oxidation.

The inhibitory effects of each aldehyde on SC and CT were evaluated by the method of Waley,[12] using Suc-Ala-Ala-Pro-Phe-PNA as substrate. The results, which showed that each aldehyde was a competitive inhibitor of both enzymes, are summarized in Table 1.

Each of the aldehydes was a significantly more potent inhibitor of CT than of SC, generally by about an order of magnitude, but by almost two orders of magnitude with (***R***)-**2** as the inhibitor. Furthermore, within each homologous series, binding of an *R*-enantiomer is stronger than for either the

(9) (a) Rawn, J. D.; Lienhard, G. E. *Biochemistry* **1974**, *13*, 3124. (b) Tatsuta, K.; Mikami, N.; Fujimoto, K.; Umezawa, S.; Umezawa, H.; Aoyagi, T. *J. Antibiot. (Tokyo), Ser. A* **1973**, *26*, 625. (c) Ito, A.; Tokawa, K.; Shimizu, B. *Biochem. Biophys., Res. Commun.* **1972**, *49*, 343. (d) Westmark, P. R.; Kelly, J. P.; Smith, B. R. *J. Am. Chem. Soc.* **1993**, *115*, 3416.

(10) Dess, D. B.; Martin, J. C. *J. Org. Chem.* **1983**, *48*, 4155.

(11) (a) Arndt, F.; Eistert, B. *Ber.* **1935**, *68*, 200. (b) Bachmann, W. E.; Struve, W. S. In *Organic Reactions;* (Florkin, M., Stotz, E. H., Eds.); Wiley and Sons Inc.: New York, 1965, Vol. 1, pp 38−62.

(12) Waley, S. G. *J. Biochem.* **1982**, *205*, 631.

corresponding *S*-enantiomer or its achiral parent, but with the variations being far greater for CT inhibition than for SC. In part, this reflects the generally weaker interactions of the inhibitors with SC. The strongest inhibition observed was of CT by (*R*)-3-phenylbutanal ((***R***)-**2**), whose K_I of 8.4 μM is 61-fold lower than that of its achiral precursor, 3-phenylpropanal (**1**), and 88-fold lower than that of its *S*-enantiomer. This 88-fold difference in CT-binding affinities between (***R***)- and (***S***)-**2**, with its unequivocal demonstration that significant discrimination of remote stereocenters is achievable using enzymes, is an extremely encouraging result. For example, if differences in binding of this magnitude were realized between diastereomeric ES complexes during catalysis of a remote stereocenter-containing racemic substrate, very high resolution efficiencies would be anticipated and the transformation would be of true asymmetric synthetic value. Even the 17.5- and 12.6-fold differences manifest between (***R***)- and (***S***)-**2** with SC and (***R***)- and (***S***)-**4** with CT, respectively, would translate into asymmetric synthetically useful distinctions for analogous remote stereocenter substrates if the overall rates of hydrolysis reflected these levels of binding disparity. Indeed, if in these cases k_{cat} variations for the enantiomeric or diastereomeric substrate transformations reinforced the binding differences to even a small degree, the degree of remote stereoselectivity discrimination achieved would become very exploitable synthetically.

The questions posed by the observed differences in binding affinities of the inhibitors **1**−**4** are intriguing. Both SC and CT appear to be largely indifferent to the presence of a methyl substituent that creates a remote stereocenter of *S*-configuration, with the K_I's of (***S***)-**2** and (***S***)-**4** with SC, and of (***S***)-**2** with CT, being so similar to those of their achiral analogs **1** and **3**, respectively. Indeed, for (***S***)-**4** with CT, the presence of the methyl group is a somewhat negative factor, with the K_I of the unsubstituted parent **3** being 5.7-fold lower. In contrast, an *R*-center methyl substituent is highly advantageous to good binding, particularly for (*R*)-3-phenylbutanal, which binds 61-fold and 16-fold more strongly with CT and SC, respectively, than does the unsubstituted inhibitor **1**. The same trend is again evident for the homologous aldehyde (***R***)-**4**, but to a lesser degree, especially for CT where the beneficial effect of the (R)-methyl group on binding is highly subdued.

Molecular modeling was applied in order to interpret the kinetic data more completely. The X-ray structures of SC and CT were energy minimized by molecular mechanics and molecular dynamics. Each aldehyde inhibitor was then docked into the active site, with the phenyl moieties in S_1, and the aldehyde carbonyl carbon covalently connected to the active site serine-CH_2OH oxygen to form the transition state-like tetrahedral intermediate. Each EI complex was then subjected to energy minimization, by molecular mechanics, followed by molecular dynamics, calculations, and the optimized conformations and the free energies of each *R*- and *S*-pair of EI complexes were compared. The results for the chiral inhibitors are depicted in Figures 2−5. The achiral inhibitors also occupied very similar active site positions. In each minimized EI complex, there were strong interactions between the oxyanion of the tetrahedral intermediate and the oxyanion hole H-bonding residues of the peptide backbone NH's of Ser195 and Gly193 of CT, and the backbone NH of Ser221 and the side chain NH_2 of Asn155 of SC, respectively.

The superimposed conformations of (*R*)- and (*S*)-3-phenylbutanal ((***R***)- **and** (***S***)-**2**) in the active site of CT (Figure 2) show that the methyl group at the stereocenter of the *R*-enantiomer is positioned in the S_2 pocket such as to elicit favorable hydrophobic interactions with the enzyme. In contrast, the

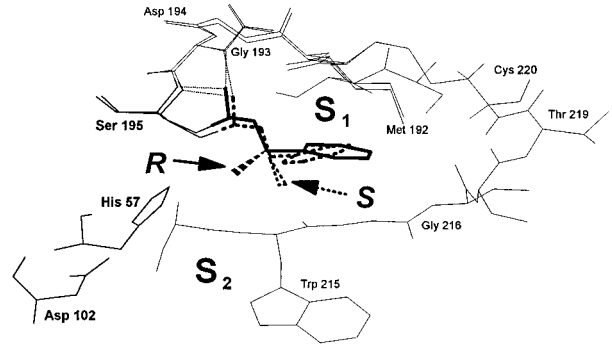

Figure 2. Superimposed energy-minimized EI complexes of (*R*)- and (*S*)-3-phenylbutanal, (***R***)-**2** (heavy solid line) and (***S***)-**2** (heavy dashed line), respectively, in the active site of CT. The oxyanions of the tetrahedral complexes derived from (***R***)-**2** and (***S***)-**2** are located in the oxyanion hole, with the negative charges stabilized by hydrogen bonding (light dashed line) with the peptide NH's of Ser195 (O^-−N = 3.18 and 3.49 Å respectively for (***R***)-**2** and (***S***)-**2**) and Gly193 (O^-−N = 2.72 and 2.79 Å respectively for (***R***)-**2** and (***S***)-**2**). Both phenyl groups are positioned in the hydrophobic S_1 pocket. The main difference between the two orientations is that the methyl group at the stereocenter of (***R***)-**2** (solid arrow) is favorably located in the S_2 pocket, while that of (***S***)-**2** (dashed arrow) is oriented toward the outside of the active site and does not contribute to binding.

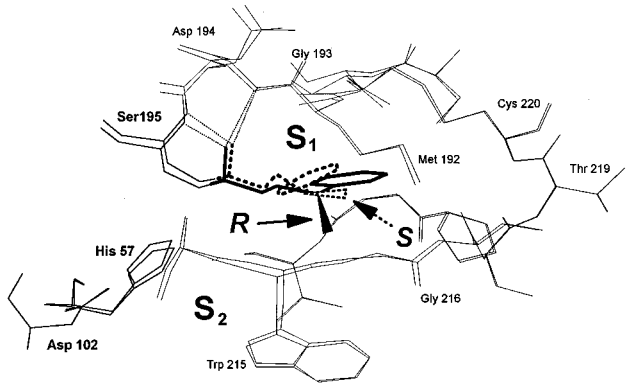

Figure 3. Superimposed energy-minimized EI complexes of (*R*)- and (*S*)-4-phenylbutanal, (***R***)-**4** (heavy solid line) and (***S***)-**4** (heavy dashed line), respectively, in the active site of CT. The oxyanions of the tetrahedral complexes derived from (***R***)-**4** and (***S***)-**4** are located in the oxyanion hole, with the negative charges stabilized by hydrogen bonding (light dashed line) with the peptide NH's of Ser195 (O^-−N = 3.00 and 3.15 Å respectively for (***R***)-**4** and (***S***)-**4**) and Gly193 (O^-−N = 2.91 and 2.84 Å respectively for (***R***)-**4** and (***S***)-**4**. The stereocenter methyl groups of both (***R***)-**4** (solid arrow) and (***S***)-**4** (dashed arrow) are obliged to locate outside of the active site and are not binding contributors. The main differences are seen to be in the locations of the phenyl groups, with that of (***R***)-**4** being positioned more deeply in the hydrophobic S_1 site than that of (***S***)-**4**.

corresponding methyl group of the *S*-enantiomer is located outside of the active site of the enzyme and is oriented toward the external water in a manner that does not contribute to hydrophobic bonding. In addition, the phenyl group of the *R*-enantiomer is able to locate itself deeper inside the hydrophobic S_1 pocket than can its enantiomeric equivalent, thereby providing a stronger phenyl-S_1 contribution to binding. It is the combination of these two factors that accounts for the dramatic 88-fold difference in K_I's between (***R***)-**2** and (***S***)-**2** as inhibitors of CT. In the cases of the homologous inhibitors, (*R*)- and (*S*)-4-phenylpentanal ((***R***)- and (***S***)-**4**), the K_I differences between inhibition of CT by the enantiomers are much smaller (12.6-fold). This also is accounted for by the molecular modeling results (Figure 3). The superimposed structures of (***R***)-**4** and (***S***)-**4** in the active site of CT reveal that the methyl

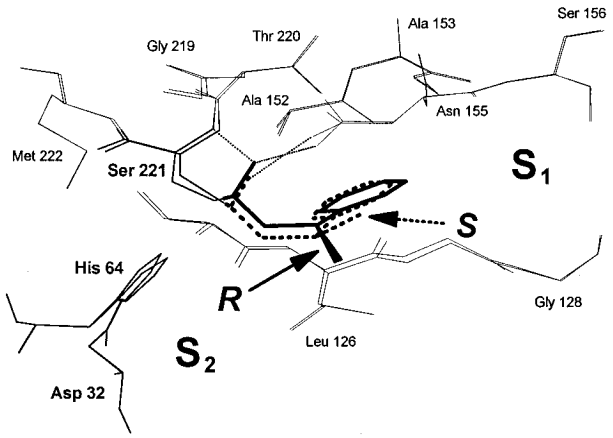

Figure 4. Superimposed energy-minimized EI complexes of (*R*)- and (*S*)-3-phenylbutanal, (***R***)-**2** (heavy solid line) and (***S***)-**2** (heavy dashed line), respectively, in the active site of SC. Both phenyl residues bind in S_1. The oxyanions of the tetrahedral complexes derived from (***R***)-**2** and (***S***)-**2** are located in the oxyanion hole, with the negative charges stabilized by hydrogen bonding (light dashed line) with the peptide NH of Ser221 and the side chain $-NH_2$ of Asn155 for (***R***)-**2** ($O^- - N$ = 2.95 and 2.72 Å respectively), but less well for (***S***)-**2**, for which only hydrogen bonding with Asn155 is seen ($O^- - N$ = 2.74 Å). The stereocenter methyl group of (***R***)-**2** (solid arrow) is oriented outside of the active site where its binding influence is neutral. In contrast, that of (***S***)-**2** (dashed arrow) takes up a position close to Asn155 and is responsible for the disruption in the oxyanion stabilization, and hence the weak overall inhibitory properties of (***S***)-**2**.

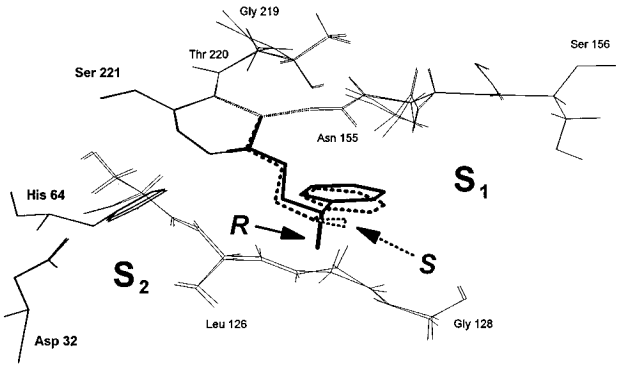

Figure 5. Superimposed energy-minimized EI complexes of (*R*)- and (*S*)-4-phenylbutanal, (***R***)-**4** (heavy solid line) and (***S***)-**4** (heavy dashed line), respectively, in the active site of SC. The oxyanions of the tetrahedral complexes derived from (***R***)-**4** and (***S***)-**4** are located in the oxyanion hole, with the negative charges similarly stabilized by hydrogen bonding (light dashed line) with the peptide NH of Ser221 ($O^- - N$ = 2.84 and 2.85 Å respectively for (***R***)-**4** and (***S***)-**4**) and the side chain $-NH_2$ of Asn155 ($O^- - N$ = 2.80 and 2.78 Å respectively for (***R***)-**4** and (***S***)-**4**). The methyl groups at the stereocenters of (***R***)-**4** (solid arrow) and (***S***)-**4** (dashed arrow) are both located outside of the active site and are non-contributors to binding. The only significant, but still minor, difference between the two EI complexes is that the phenyl group of (***R***)-**4** penetrates more deeply into the hydrophobic S_1 region than does that of (***S***)-**4**.

groups of both the *R*- and *S*-enantiomers are directed toward the outside of the active site. The *S*-enantiomer is obliged to adopt this unusual orientation in order to avoid unfavorable steric interactions between the methyl group and the side chain of Met 192. As a consequence, this prevents the phenyl group of (***S***)-**4** from penetrating as deeply into the hydrophobic S_1 pocket as it might otherwise, thereby precluding the strong phenyl$-S_1$ hydrophobic interactions that (***R***)-**4** enjoys. The latter enantiomer does not bind as strongly as (***R***)-**2** above because it lacks the strong hydrophobic bonding contribution that the additional methyl$-S_2$ interaction provides in the Figure 2 situation.

The molecular modeling results on the SC inhibitors are equally enlightening. The superimposed structures of (*R*)- and (*S*)-3-phenylbutanal ((***R***)- and (***S***)-**2**) in their EI-complexes with SC are depicted in Figure 4. In both complexes, the phenyl residues of both (***R***)-**2** and (***S***)-**2** penetrate adequately, and almost equivalently, into S_1 to provide good hydrophobic binding contributions to the corresponding K_I's. For the (***R***)-**2** orientation, the methyl group at the stereocenter is oriented toward the outside of the active site and does not make any binding contribution. In contrast to this neutral binding role, the position that the (***S***)-**2** methyl group is obliged to occupy elicits unfavorable steric interactions of the methyl group with the Asn155 oxyanion hole residue. As a result, the usual oxyanion stabilization mechanism is disturbed. For example, the distances between the oxyanion of the *S*-enantiomer and the backbone *N* and N*H* of Ser 221 have become 3.95 and 3.15 Å, respectively, which precludes normal oxyanion hydrogen bonding. Thus the EI complex of (***R***)-**2** with SC is relatively favored over that of (***S***)-**2** by the absence of negative interactions rather than, as in the case of CT (Figure 2), of a beneficial contribution by the methyl substituent. For the interactions of the higher homologue inhibitors (*R*)- and (*S*)-4-phenylpentanal ((***R***)- and (***S***)-**4**) with SC, the minor (4.8-fold) K_I variations and the relatively weak binding of each enantiomer indicate that there should be little difference in their orientations in the active site, and that there are no strong EI interactions. This is confirmed by the minimized complexes of Figure 5, in which the phenyl groups of both (***R***)- and (***S***)-**4** are similarly, but not deeply, located in S_1, and with the methyl groups at the stereocenter both oriented away from the active site into locations that influence binding neither favorably nor adversely.

A comparison of $\Delta\Delta G^{\ddagger}$ values for the inhibition of CT and SC provides further support for the validity of the molecular modeling analyses of the weaker *R*- and *S*-stereocenter discrimination for structures **4** than for **2**. The differences in experimental (from K_I's) and calculated (from EI-complex energies) $\Delta\Delta G^{\ddagger}$'s for the ***R***- and ***S***-pairs of **2** and **4** are similar, each being 50−70% lower for (***R***)- and (***S***)-**4** than for (***R***)- and (***S***)-**2** for both CT and SC.

While the current results represent only a first step toward probing remote stereocenter stereoselectivity of enzymes, the strategy of using competitive inhibitors is clearly an effective one. The observation that the stereocenters of **2** and **4** become less well recognized the more distant they are from the site of reaction is in accord with the established trend in asymmetric catalysis generally.[3] Thus in attempting to establish enzymatic control of the configurations of remote stereocenters, the natural proclivity of enzymes to manifest maximum stereoselectivity close to the catalytic site will have to be conquered. Another of our ultimate goals is to formulate guidelines for forecasting the degrees of stereocenter discrimination to be expected in the transformations of any new, unnatural substrate structures catalyzed by synthetically useful enzymes. In this regard, the molecular modeling results are encouraging in that the differences in calculated binding energies for enantiomeric pairs studied here are proportional to the actual differences in K_I's. If this promise holds out, it will be possible to develop protocols for rapidly screening remote-stereocenter, synthon-precursor, structures of interest, using calculations of their relative energies of binding to appropriate enzymes as a basis for predicting whether significant stereocenter discrimination will be attainable, and hence identifying the most favorable enzyme−substrate combination for asymmetric synthetic use. Further studies toward these objectives, using an expanded structural range of inhibitors as probes, are in hand.

Experimental Section

General Methods. Anhydrous reagents were prepared according to the literature procedure.[13] Analytical TLC was performed on precoated plates (silica gel 60F-254). Purification by radial TLC was performed on a model 7924T Chromatotron from Harrison Research. Plates of 4 and 2 mm thickness were coated with E. Merck Silica Gel 60 PF254 containing gypsum. Absorption measurements were performed on a Perkin Elmer Lambda 2 UV/vis spectrometer. IR spectra were determined on films on a Nicolet 5DX FTIR spectrophotometer. NMR (^{1}H, ^{13}C) spectra were recorded on a Gemini 200 (200, 50 MHz, respectively) spectrometer. ^{1}H NMR chemical shifts are reported in ppm relative to the TMS peak ($\delta = 0.0$) with $CDCl_3$ as solvent. ^{13}C NMR chemical shifts are reported in ppm relative to the $CDCl_3$ peak ($\delta = 77.0$) with $CDCl_3$ as solvent. Optical rotations were measured on a Perkin-Elmer 141 polarimeter. Mass spectra were measured on a Bell and Howell 21−490 (low resolution) or an AEI MS3074 instrument (high resolution).

Reagent grade chemicals, 3-phenylpropanal (**1**), 4-phenylbutan-1-ol, (±)-3-phenylbutanoic acid, (*R*)-(+)-α-methylbenzylamine (96% *ee*), (*S*)-(−)-α-methylbenzylamine (99% *ee*), Diazald (*N*-methyl-*N*-nitroso-*p*-toluenesulfonamide), and diisobutylaluminum hydride (DIBAL, 1.0 M in CH_2Cl_2) were purchased from Aldrich. Subtilisin Carlsberg (EC 3.4.21.14), α-chymotrypsin (EC 3.4.21.1), and succinyl-*L*-Ala-*L*-Ala-*L*-Pro-*L*-Phe-*p*-nitroanilide (Suc-Ala-Ala-Pro-Phe-PNA) were purchased from Sigma Chemical Co. The concentration of SC was estimated by the rate of the hydrolysis of Suc-Ala-Ala-Pro-Phe-PNA.[14] The concentration of CT was estimated by the rate of the hydrolysis of *p*-nitrophenyl acetate.[15] The Dess−Martin reagent[10] and (*S*,*S*)-*N*,*N*′-dimethyl-1,2-diphenylethylenediamine[16,17] were prepared according to the literature procedure.

Resolution of (±)-3-Phenylbutanoic acid. (±)-3-Phenylbutanoic acid was resolved with (*R*)-(+)-α-methylbenzylamine to give (*R*)-(−)-3-phenylbutanoic acid (42%): $[\alpha]^{20}_D$ −29.4° (*c* 1.3, EtOH); lit.[18] $[\alpha]^{25}_D$ −58.5° (*c* 3.0, benzene). (*S*)-(+)-3-Phenylbutanoic acid (30%) was obtained similarly using (*S*)-(−)-α-methylbenzylamine: $[\alpha]^{20}_D$ +29.1° (*c* 1.2, EtOH); lit.[19] $[\alpha]^{25}_D$ +54.4° (*c* 1.4, benzene).

***(R)*-(−)-3-Phenylbutanal ((*R*)-2)** To a solution of (*R*)-(−)-3-phenylbutanoic acid (500 mg, 3.0 mmol) in Et_2O (20 mL) at 20 °C was added an ethereal solution of CH_2N_2, generated from Diazald, until the reaction mixture became yellow. The reaction mixture was stirred for additional 2 h at 20 °C and concentrated under reduced pressure. The residue was chromatographed on silica gel (hexanes), and methyl (*R*)-(−)-3-phenylbutanoate (490 mg, 91%) was obtained as a colorless oil: $[\alpha]^{20}_D$ −35.7° (*c* 2.2, EtOH); ^{1}H NMR δ 1.30 (3H, d, $J = 7.0$ Hz), 2.50−2.70 (2H, m), 3.20−3.40 (1H, m), 3.62 (3H, s), 7.15−7.37 (5H, m).

DIBAL (1.0 M solution in CH_2Cl_2, 2.6 mmol, 2.1 mol equiv) was added dropwise under an N_2 atmosphere at −78 °C to a solution of methyl (*R*)-(−)-3-phenylbutanoate (215 mg, 1.2 mmol, 1.0 mol equiv) in CH_2Cl_2 (10 mL). The reaction mixture was stirred for 2 h at −78 °C, then slowly warmed to 20 °C and stirred for an additional 12 h at 20 °C. The reaction was quenched by the addition of MeOH (3 mol equiv), the aluminum oxide removed by filtration through Celite, and the filtrate concentrated under reduced pressure. The residue was dissolved in hexanes (10 mL), filtered through a small silica gel column, and concentrated to give (*R*)-(−)-3-phenylbutan-1-ol (165 mg, 91%) as a colorless oil, which was used without further purification: ^{1}H NMR δ 1.28 (3H, d, $J = 7.0$ Hz), 1.35−1.45 (1H, br), 1.81−1.92 (2H, m), 2.78−2.98 (1H, m), 3.45−3.65 (2H, m), 7.15−7.37 (5H, m).

To a solution of the Dess−Martin reagent (440 mg, 1.0 mmol, 1.2 mol equiv) in CH_2Cl_2 (5.0 mL) was added (*R*)-(−)-3-phenylbutan-1-ol (120 mg, 0.87 mmol, 1.0 mol equiv) in CH_2Cl_2 (2.0 mL) at 20 °C. The reaction mixture was stirred for 30 min at 20 °C, then diluted with Et_2O (7.0 mL) and poured into sodium thiosulfate (1.1 g, 7.0 mol equiv) in saturated aqueous $NaHCO_3$ (20 mL) and stirred for 10 min. The layers were separated, and the organic layer was washed sequentially with saturated aqueous $NaHCO_3$ and deionized water. The combined organic layers were dried ($MgSO_4$), filtered, and concentrated under reduced pressure. The crude product was purified by radial TLC (Chromatotron, hexanes/EtOAc, 9:1) to give (*R*)-(−)-3-phenylbutanal ((***R*)-2,** 120 mg, 94%, >95% *ee*) as a colorless oil: $[\alpha]^{25}_D$ −38.5° (*c* 0.2 g, Et_2O); lit.[20] $[\alpha]^{25}_D$ −38.0° (*c* 0.2, Et_2O); ^{1}H NMR δ 1.32 (3H, d, $J = 7.0$ Hz), 2.55−2.85 (2H, m), 3.25−3.45 (1H, m), 7.18−7.37 (5H, m), 9.71 (1H, t, $J = 2.0$ Hz).

The preparation of **(***S*)-(+)-3-phenylbutanal ((***S*)-2)** was carried out in the same manner, as follows:

(*S*)-(+)-3-Phenylbutanal ((*S*)-2). (*S*)-(+)-3-Phenylbutanoic acid (520 mg, 3.2 mmol) and CH_2N_2 in Et_2O gave methyl (*S*)-(+)-3-phenylbutanoate (560 mg, 98%): $[\alpha]^{20}_D$ +35.2° (*c* 2.2, EtOH), spectroscopically identical to the *R*-enantiomer.

Methyl (*S*)-(+)-3-phenylbutanoate (500 mg, 2.8 mmol, 1.0 mol equiv) and DIBAL (1.0 M solution in CH_2Cl_2, 6.0 mmol, 2.1 mol equiv) yielded (*S*)-(+)-3-phenylbutan-1-ol (410 mg, 98%), spectroscopically identical with the *R*-enantiomer.

(*S*)-(+)-3-Phenylbutanol (410 mg, 2.7 mmol, 1.0 mol equiv) and the Dess−Martin reagent (1.4 g, 3.3 mmol, 1.2 mol equiv) afforded (*S*-(+)-3-phenylbutanal ((***S*)-2**, 330 mg, 82%, >95% *ee*): $[\alpha]^{25}_D$ +37.1° (*c* 0.2, Et_2O); lit.[20] $[\alpha]^{25}_D$ +38.0° (*c* 0.2, Et_2O), spectroscopically identical to (***R*)-2**.

4-Phenylbutanal (3). 4-Phenylbutan-1-ol (700 mg, 4.7 mmol, 1.0 mol equiv) was oxidized with the Dess−Martin reagent (2.4 g, 5.7 mmol, 1.2 mol equiv) in CH_2Cl_2 (35 mL). After workup and purification using the Chromatotron (hexanes/EtOAc, 90/10), 4-phenylbutanal[21] (**3**, 575 mg, 83%) was obtained as a colorless oil: ^{1}H NMR δ 1.90−2.05 (2H, m), 2.35−2.50 (2H, m), 2.62−2.75 (2H, m), 7.15−7.35 (5H, m), 9.76 (1H, t, $J = 1.5$ Hz).

(*R*)-(−)-4-Phenylpentanal (*R*-4). (*R*)-(−)-3-phenylbutanoic acid (520 mg, 3.1 mmol, 1.0 mol equiv) was dissolved in thionyl chloride (754 mg, 6.34 mmol, 2.0 mol equiv) under an N_2 atmosphere and the reaction mixture was refluxed for 2 h to remove of the excess thionyl chloride under reduced pressure, followed by Kugelrohr distillation, to give (*R*)-(−)-3-phenylbutanoyl chloride (560 mg, 97%) as a colorless oil, which was used directly.

(*R*)-(−)-3-Phenylbutanoyl chloride (560 mg, 3.1 mmol, 1.0 mol equiv) in Et_2O (5.0 mL) was added dropwise at 0 °C to a solution of CH_2N_2 (generated from Diazald (2.0 g, 9.3 mmol, 3.0 mol equiv)), in Et_2O (25 mL), and the reaction mixture was then stirred at 20 °C for 3 h. The reaction mixture was then concentrated under reduced pressure and the crude product purified by Chromatotron chromatography (hexanes/EtOAc, 9:1) to give (*R*)-(−)-1-diazo-4-phenylpentan-2-one (566 mg, 97%) as a yellow oil: $[\alpha]^{25}_D$ −109° (*c* 0.5, CH_2Cl_2); IR (cm^{-1}) 3081, 2968, 2105, 1639; ^{1}H NMR δ 1.31 (3H, d, $J = 7.0$ Hz), 2.45−2.70 (2H, m), 3.20−3.40 (1H, m), 5.10 (3H, s), 7.15−7.37 (5H, m); ^{13}C NMR δ 21.7, 36.5, 49.2, 54.9, 126.3, 126.6, 128.4, 145.7, 193.6.

To a solution of (*R*)-(−)-1-diazo-4-phenylpentan-2-one (495 mg, 2.6 mmol) in methanol (19 mL) was added a catalytic amount of Ag_2O at 60 °C. After N_2 evolution ceased (5 min), the reaction mixture was stirred an additional 30 min at 60 °C, Norit was added, and the reaction mixture was filtered, concentrated under reduced pressure, and purified by Chromatotron (hexanes) to give methyl (*R*)-(−)-4-phenylpentanoate (418 mg, 83%) as a colorless oil: $[\alpha]^{25}_D$ −22.0° (*c* 1.1, CH_2Cl_2); IR (cm^{-1}) 3061, 2959, 1735, 1605; ^{1}H NMR δ 1.27 (3H, d, $J = 6.9$ Hz), 1.85−2.00 (2H, m), 2.15−2.27 (2H, m), 2.62−2.82 (1H, m), 3.63 (3H, s), 7.15−7.37 (5H, m); ^{13}C NMR δ 22.2, 32.3, 33.2, 39.4, 51.4, 126.1, 126.9, 128.4, 146.1, 173.0.

(13) 13)Perrin, D. D.; Armarego, W. L. F.; Perrin, D. R. *Purification of Laboratory Chemicals*; Pergamon Press: New York, 1980.

(14) (a) Del Mar, E. G.; Largman, C.; Brodricl, J. W.; Goekas, M. C. *Anal. Biochem.* **1979**, *99*, 316. (b) Russell, A. J.; Thomas, P. G.; Fersht, A. R. *J. Mol. Biol.* **1987**, *193*, 803.

(15) (a) Kezdy, F. J.; Kaiser, E. T. *Methods Enzymol.* **1970**, *19*, 3. (b) Ottensen, M.; Svendsen, I. *Methods Enzym. Anal.* **1984**, *5*, 159.

(16) Mangeney, P.; Tejero, T.; Alexakis, A.; Grosjean, F.; Normant, J. *Synthesis* **1988**, 255.

(17) Mangeney, P.; Grosjean, F.; Alexakis, A.; Normant, J. *Tetrahedron Lett.* **1988**, *29*, 2675.

(18) Cram, D. J. *J. Am. Chem. Soc.* **1952**, *74*, 2137.

(19) Sorlin, G.; Bergson, G. *Ark. Kemi* **1968**, *29*, 593.

(20) Mangeney, P.; Alexakis, A.; Normant, J. F. *Tetrahedron Lett.* **1988**, *29*, 2677.

(21) 4-Phenylbutanal had been synthesized by different methods: (a) Kumler, W. D.; Strait, L. A.; Alpen, E. L. *J. Am. Chem. Soc.* **1950**, *72*, 1463. (b) Braun, J. V. *Chem. Ber.* **1934**, *67*, 218.

The same reduction and oxidation procedure used above to prepare (***R***)-**2** was then followed. Methyl (*R*)-(−)-4-phenylpentanoate (360 mg, 1.9 mmol, 1.0 mol equiv) and DIBAL (1.0 M solution in CH_2Cl_2, 4.2 mmol, 2.2 mol equiv) gave (*R*)-(−)-4-phenylpentan-1-ol (270 mg, 88%): IR (cm^{-1}) 3339 (br), 3060, 2932, 1603; ^1H NMR δ 1.26 (3H, d, J = 6.9 Hz), 1.40−1.80 (6H, m), 2.60−2.80 (1H, m), 3.59 (2H, t, J = 6.4 Hz), 7.15−7.35 (5H, m); ^{13}C NMR δ 22.4, 30.9, 34.4, 39.8, 62.9, 125.8, 126.9, 128.3, 147.2.

(*R*)-(−)-4-Phenylpentanol (253 mg, 1.6 mmol, 1.0 mol equiv) and the Dess−Martin reagent (1.0 g, 2.3 mmol, 1.5 mol equiv) yielded (*R*)-(−)-4-phenylpentanal ((***R*)-4,**160 mg, 63%, >95% *ee*): $[\alpha]^{25}_D$ −16.2° (*c* 0.9, CH_2Cl_2); IR (cm^{-1}) 3064, 2967, 1724, 1603; ^1H NMR δ 1.28 (3H, d, J = 7.0 Hz), 1.80−2.00 (2H, m), 2.27−2.40 (2H, m), 2.62−2.80 (1H, m), 7.15−7.37 (5H, m), 9.69 (1H, t, J = 1.5 Hz); ^{13}C NMR δ 22.2, 30.3, 39.2, 42.1, 126.2, 126.8, 128.4, 145.9, 202.1; HRMS, calcd for M^+ $C_{11}H_{14}O$ *m/e* 162.1045, found *m/e* 162.1051.

The preparation of (*S*)-(+)-4-phenylpentanal **(((*S*)-4)** was carried out in the same manner, as follows:

(*S*)-(+)-4-Phenylpentanal ((*S*)-4). (*S*)-(+)-3-Phenylbutanoic acid (380 mg, 2.31 mmol, 1.0 mol equiv) and thionyl chloride (540 mg, 4.62 mmol, 2.0 mol equiv) gave (*S*)-(+)-3-phenylbutanoyl chloride (403 mg, 95%).

(*S*)-(+)-3-phenylbutanoyl chloride (403 mg, 2.2 mmol, 1.0 mol equiv) and CH_2N_2 (from Diazald (1.41 g, 6.6 mmol, 3.0 mol equiv)) afforded (*S*)-(+)-1-diazo-4-phenylpentan-2-one (356 mg, 87%): $[\alpha]^{25}_D$ +107° (*c* 0.5, CH_2Cl_2); spectroscopically identical to the *R*-enantiomer.

(*S*)-(+)-1-Diazo-4-phenylpentan-2-one (300 mg, 1.6 mmol), Ag_2O (catalytic), and MeOH (13 mL) yielded methyl (*S*)-(+)-4-phenylpentanoate (250 mg, 82%): $[\alpha]^{25}_D$ +22.2° (*c* 1.0, CH_2Cl_2), spectroscopically identical to the *R*-enantiomer.

Methyl (*S*)-(+)-4-phenylpentanoate (167 mg, 0.9 mmol, 1.0 mol equiv) and DIBAL (1.0 M solution in CH_2Cl_2, 1.9 mmol, 2.2 mol equiv) gave (*S*)-(+)-4-phenylpentan-1-ol (135 mg, 95%), spectroscopically identical to the *R*-enantiomer.

(*S*)-(+)-4-Phenylpentan-1-ol (140 mg, 0.86 mmol, 1.0 mol equiv) and the Dess−Martin reagent (550 mg, 1.3 mmol, 1.5 mol equiv) yielded (*S*)-(+)-4-phenylpentanal **((*S*)-4,** 85 mg, 60%, >95% *ee*): $[\alpha]^{25}_D$ +16.7° (*c* 0.9, CH_2Cl_2), spectroscopically identical to (***R*)-4**. HRMS, calcd for M^+ $C_{11}H_{14}O$ *m/e* 162.1045, found *m/e* 162.1049.

General Procedure for the Determination of Enantiomeric Excess. To a solution of aldehyde ((***R*,*S*)-2** and (***R*,*S*)-4**, 0.15 M, 1.0 mol equiv) in Et_2O was added molecular sieves followed by (*S*,*S*)-*N*,*N*′-dimethyl-1,2-diphenyl-ethylenediamine (1.3 mol equiv) at 20 °C under N_2. The reaction mixture was stirred for 5 h at 20 °C and then filtered through Celite. The filtrate was concentrated *in vacuo*, and the ^{13}C NMR spectrum of the residue was taken. The integrations of the peaks for the methyl groups at the stereocenters of each aldehyde (22.21 ppm for (***R*)-2**, 24.60 ppm for (***S*)-2**, 22.52 ppm for (***R*)-4**, and 22.90 ppm for (***S*)-4**) were used to determine the enantiomeric excesses. In each case, the materials were seen to be enantiomerically pure, within the ±5% confidence limits of the NMR method.

Kinetic Measurements. The enzyme kinetics for both SC and CT were performed at 25 °C by measuring the absorbance of the PNA (ϵ = 8800 at 410 nm) released during the hydrolysis of Suc-Ala-Ala-Pro-Phe-PNA. All kinetic runs were carried out in duplicate. For SC, K_M and k_{cat} of Suc-Ala-Ala-Pro-Phe-PNA were determined by measuring initial rates of hydrolysis at different substrate concentrations (0.031, 0.042, 0.067, 0.125, 0.250, 0.500, 1.000, 2.000 mM), and fitting the obtained data to the Michaelis-Menten equation using the Grafit program (version 3.0, Erithacus Software Ltd., UK). Assays were run in 0.1 M sodium phosphate buffer at pH 7.5, containing 0.5 M NaCl, and 5% (v/v) dimethyl sulfoxide. The enzyme concentration was 0.47 nM. The K_I for each inhibitor for SC was determined by Waley's method.[12] The progress curve without inhibitor was obtained from an assay mixture containing 0.2 M NaH_2PO_4 and 1.0 M NaCl (1.47 mL), pH 7.5 buffer with 0.1 M NaH_2PO_4 (50 μL), 1.0 M NaCl (30 μL), 25 mM substrate in DMSO (30 μL), DMSO (120 μL), and H_2O (1.29 mL). This mixture was incubated in a water jacket for 5 min at 25 °C prior to initiation of the reaction by addition of 10 μL of SC stock solution (1.4×10^{-6} M in 0.1 M NaH_2PO_4 buffer, pH 7.5). The final volume of the assay mixture was 3 mL, with a final concentration of 0.1 M NaH_2PO_4, 0.5 M NaCl, 4.5 nM of the enzyme, 0.25 mM of substrate, and 5% DMSO. The progress curve with inhibitor was obtained similarly, but with 10−120 μL of the inhibitor solution (0.14−0.27 M in DMSO) added. The progress of each hydrolysis was recorded directly into a PC. Points for calculation[12] were taken at 15,18, 21, 24, 27, 30, 33, 36, and 39% conversions.

All kinetic measurements for CT were performed with degassed water to minimize the inhibition of the enzyme by CO_2, and the kinetic determinations were carried out as described above for SC. K_M and k_{cat} values for Suc-Ala-Ala-Pro-Phe-PNA were determined (Grafit) for the following assay conditions: substrate concentration (0.025, 0.033, 0.050, 0.100, 0.200, 0.500, and 1.000 mM), 0.1 M NaH_2PO_4 buffer (pH 7.5), 0.5 M NaCl, 5% DMSO, and 2.1 nM of CT. The progress curve without inhibitor was obtained from an assay mixture containing 0.2 M NaH_2PO_4 (pH 7.5) and 1.0 M NaCl (1.50 mL), 25 mM substrate in DMSO (30 μL), DMSO (120 μL), and H_2O (1.32 mL) which was incubated in a water jacket for 5 min at 25 °C prior to initiation of the reaction by the addition of 30 μL of CT stock solution (1.6×10^{-6} M in 1.0 mM HCl). The final volume of the assay mixture was 3 mL with a final concentration of 0.1 M NaH_2PO_4, 0.5 M NaCl, 16 nM of the enzyme, 0.25 mM of substrate, and 5% DMSO. The progress curve with inhibitor was obtained similarly, with 100−120 μL of the inhibitor solution (0.14−0.17 M in DMSO) added. The progress of hydrolysis was recorded directly into a PC. The inhibition constants were determined as described for SC. The results are recorded in Table 1.

Computational Methods. System Setup. The reference structures used for SC[5a] and CT[5d] were from the Protein Data Bank[22] at Brookhaven National Laboratory,[23] with Insight II (version 2.3.0, Biosym Technologies, Inc., San Diego, CA, USA) as the graphics software on a Silicon Graphics Indigo computer. To create initial coordinates for the minimization of SC, the inhibitor (eglin C) and the three calcium ions were removed. Hydrogens were added at the pH (7.5) used for the kinetic measurements, which protonated all Lys and Arg side chains, and the N-terminal NH_2, and deprotonated all Glu and Asp side chains, and the C-terminal COOH. The overall charge of the enzyme resulting from this setup was −1. To complete the setup, only crystallographic water molecules within 5 Å from the enzyme surface were maintained and a 5-Å shell of water was generated to surround the enzyme. The total number of water molecules in this setup was 1274. In the case of CT the dimeric structure of the enzyme was split into its individual, independent, monomers, and only one of the monomers used to create the initial coordinates. The missing residues Gly 12 and Leu 13 were added using Insight. The setup was then completed as reported above for SC. The final charge of the molecule was +2, and the total number of water molecules was 1252. Minimizations of each enzyme were performed with the DISCOVER program (Biosym, Version 3.1) using the Consistent Valence Force Field (CVFF).[24] The nonbonded pair list was updated every 20 cycles and a dielectric constant of 1 was used in all calculations. A switching function was used to scale down the electrostatic and the van der Waals interactions from full to zero between 10 and 12 Å, with a nonbonded cutoff of 14 Å. The energy of the system was minimized with respect to all 3*N* Cartesian coordinates until the maximum derivative of 0.1 kcal/(mol·Å) was reached. The minimized enzyme structures obtained were then used as the bases for the molecular mechanics calculations on enzyme−inhibitor complexes

Energy Minimizations of Enzyme−Inhibitor Complexes. For SC, to set up the initial structure for the energy minimization on each inhibitor, the carbonyl carbon was covalently bound to the oxygen of the hydroxyl group of the active site Ser221 of SC to form the oxyanion-containing tetrahedral intermediate. The hydrogen atom of the Ser221 hydroxyl group was then transferred to the sp^2 nitrogen of the imidazole ring of the side chain of His64, rendering it positively charged. The

(22) For subtilisin Carlsberg entry 2SEC, 1.8-Å resolution; for α-chymotrypsin entry 4CHA, 1.68-Å resolution.

(23) (a) Bernstein, F. C.; Koetzle, T. F.; Williams, J. B.; Meyer, E. F., Jr.; Brice, M. D.; Rogers, J. R.; Kennard, O.; Shimanouchi, T.; Tasumi, M. *J. Mol. Biol.* **1977**, *112*, 535. (b) Abola, E. E.; Bernstein, F. C.; Bryant, S. H.; Koetzle, T. F.; Weng, J. In *Crystallographic Databases—Information Content, Software Systems, Scientific Applications*; Allen, F. H., Bergerhoff, G., Sievers, R., Eds; Data Commision of the International Union of Crystallography: Bonn/Cambridge/Chester, 1987, 107.

(24) Hagler, A. T.; Osguthorpe, D. J.; Dauber-Osguthorpe, P.; Hempel, J. C. *Science* **1985**, *227*, 1309.

X-ray structure of the Met192Ala mutant of α-lytic protease complexed with methoxysuccinyl-Ala-Ala-Pro-phenylalanylboronic acid[25] was used as the model for docking the tetrahedral intermediate into the active site of SC. The oxyanion was oriented toward the oxyanion hole, formed by the side chain NH_2 of Asn155 and the backbone NH of Ser221. The aromatic residue of each inhibitor was positioned in the S_1 pocket, defined by Ser125−Ala129, Ala152−Ser156, and Ile165−Tyr167 in a manner that avoided all bad Van der Waals interactions. At this time, six water molecules in the SC active site that were located in positions that caused severe steric interactions with the docked inhibitor were removed.

An analogous docking procedure was used for CT. The reference structure used for docking was that of CT complexed with 2-phenylethylboronic acid.[5g] The oxyanion of the tetrahedral intermediate generated by attack of the active site Ser195 was directed toward the oxyanion hole formed by the backbone NH's of Gly193 and Ser195, and a positive charge was generated on His57 by transferring the hydrogen from the Ser195 hydroxyl group. The aromatic ring of each inhibitor was positioned in the S_1 pocket, defined by Val213−Thr219, Ser190−Asp194, Ser189, and Gly226. Again, six water molecules located too close to the inhibitor were also removed from the CT active site.

The partial charges on the active site serine and the enzyme-bound aldehyde complex were generated by a semiempirical *ab initio* calculation program (Mopac, Biosym). The overall negative charge of −1 was distributed between the oxygen atoms bound to the tetrahedral carbon formed from aldehyde. The partial charges of residues His64 for SC and His57 for CT were assigned as reported.[26]

For running the energy minimization, the same strategy was applied for both SC and CT by using a nonbonded cutoff of 14 Å, with a switching function between 10 and 12 Å. All residues and the water molecules located outside of the cutoff distance were fixed to reduce the computation time while the enzyme-bound inhibitor and the water molecules within the cutoff distance were free to move throughout the calculation. Initially, all heavy atoms on the enzyme were tethered using harmonic restraints, and the energy minimized with respect to the positions of the hydrogen atoms, using steepest descents, until the maximum derivative was <0.5 kcal/(mol·Å). The restraints were then applied only to the heavy atoms on the main chain, and the minimization continued, again using steepest descents, until the maximum derivative was <0.25 kcal/(mol·Å). Finally, the restraints were removed from all atoms, and the energy minimized using steepest descents until the maximum derivative was <0.1 kcal/(mol·Å), and then using conjugate gradients until the maximum derivative was <0.01 kcal/(mol·Å).

The resulting enzyme−inhibitor structure was used as the starting point for the molecular dynamics calculations. During the molecular dynamic simulations, the whole enzyme was kept fixed, as were water molecules more than 14 Å away from Ser221 of SC or Ser195 of CT. The molecular dynamic simulations were performed at 500 °K, at a time step of 1 fs, and sampling every 10 steps over a 10 ps time period. As an additional comparison, the lowest energy structure from the molecular dynamics simulation was reminimized by molecular mechanics as described above. In each case, the latter structures were found to be almost identical with those of the initial, molecular mechanics-minimized structures. For the enzyme−inhibitor complexes of **(*R*)-2**−**(*S*)-2** and **(*R*)-4**−**(*S*)-4** with CT, the calculated $\Delta\Delta G^{\ddagger}$ values were 6.4 and 4.5 kcal/mol, respectively, and for SC, 5.3 and 3.2 kcal/mol, respectively. The corresponding experimental $\Delta\Delta G^{\ddagger}$ values were 2.7 and 1.3, and 1.7 and 0.93 kcal/mol, respectively.

Acknowledgment. Support from the Natural Sciences and Engineering Research Council of Canada and the award of University of Toronto Open Scholarships (to T.L.) are gratefully acknowledged.

Supporting Information Available: ^1H and ^{13}C NMR spectra of (***R***)- and (***S***)-**4** (4 pages). This material is contained in many libraries on microfiche, immediately follows this article in the microfilm version of the journal, can be ordered from the ACS, and can be downloaded from the Internet; see any current masthead page for ordering information and Internet access instructions.

JA952835T

(25) Bone, R.; Silen, J. L.; Agard, D. A. Entry 1P08 in the Brookhaven protein database, 2.25-Å resolution.

(26) Rao, S. N.; Singh, U. C.; Bash, P. A.; Kollman, P. A. *Nature* **1987**, *328*, 551.